

Formation of Platinum Sites on Layered Double Hydroxide Type Basic Supports: II. Effect of the Nature of the Interlayer Anion of the Layered Aluminum–Magnesium Hydroxides on Platinum Binding and Pt/MgAlO_x Formation

O. B. Belskaya^{a, b}, T. I. Gulyaeva^a, N. N. Leont'eva^a, V. I. Zaikovskii^c,
T. V. Larina^c, T. V. Kireeva^a, V. P. Doronin^{a, b}, and V. A. Likholobov^{a, b}

^a Institute of Hydrocarbons Processing, Siberian Branch, Russian Academy of Sciences, Omsk, 644040 Russia

^b Omsk State Technical University, Omsk, 644050 Russia

^c Boreskov Institute of Catalysis, Siberian Branch, Russian Academy of Science, Novosibirsk, 630090 Russia

e-mail: obelska@ihcp.oscsbras.ru

Received June 17, 2010

Abstract—The interaction of aqueous H₂PtCl₆ solutions with hydrotalcite-type aluminum–magnesium hydroxides differing in the nature of their interlayer anion is reported. In the case of CO₃²⁻ as the interlayer anion, the introduction of the platinum(IV) chloro complex does not exert a significant effect on the structural properties of the support, on its thermal decomposition dynamics, and on the textural characteristics of the resulting oxide phase. The binding of the platinum complexes to “activated hydrotalcite” with interlayer OH⁻ anions increases the interplanar spacing and enhances the thermal stability of the layered structure. This is accompanied by marked changes in textural characteristics of the material, leading to the formation of a nearly monodisperse mixed oxide phase. In the Pt/MgAlO_x samples obtained by reductive treatment, a considerable proportion of platinum is in the form of planar particles, and this corroborates the hypothesis that the metal complex at the sorption stage is mainly localized in the interlayer space of this support. Platinum binds to the support as chloro complexes via rapid anion exchange, and these bound platinum species are characterized by a higher reduction temperature.

DOI: 10.1134/S0023158411060036

Hydrotalcite-type layered double hydroxides are promising supports for metal catalysts. Introduction of a metal significantly changes the properties of the hydroxide phase and of the mixed oxide resulting from heat treatment: it enhances the catalytic activity of the hydroxide in a number of reactions [1, 2] and raises its acid gas adsorption capacity [3–5].

Most studies in this field are devoted to the introduction of nickel, which is capable of isomorphically replacing part of the magnesium in the brucite layers of the layered structure [6]. The main ways of introducing nickel are the template method (coprecipitation of magnesium and aluminum hydroxides and a nickel compound) and ion exchange. In the ion exchange method, nickel is introduced in cationic form via partial substitution for magnesium or aluminum in the brucite layers or in anionic form via replacement of interlayer anions. Platinum metals are commonly supported by incipient-wetness impregnation using a minimum possible amount of a solution, without controlling the processes involved in the binding of the metal [5, 7, 8]. These metals are also supported by deposition of their hydrolyzed species [9]. Metal com-

plexes are often deposited from their toluene solutions. This does not cause any restructuring support, does not modify its acid–base properties, and minimizes the interaction between the catalyst precursor and the support [3, 7, 10]. The exchange of interlayer anions is considered in a few works dealing with the anion-exchange properties of hydrotalcite-like compounds [8, 11]. However, this process has practically not been investigated from the standpoint of introducing anionic species of the precursor of the active component of the catalyst.

Here, we report the interaction of aqueous solutions of anionic Pt(IV) chloro complexes with layered double hydroxides during the synthesis of Pt/MgAlO_x catalysts. The precursors of the aluminum–magnesium oxide supports were layered hydroxides containing carbonate or hydroxide anions in their interlayer space (HT-CO₃ and HT-OH, respectively). Our detailed study of these hydroxide supports [12] demonstrated that the morphology of the layered particles and the nature of the interlayer anion determine the oxide support structure formation conditions and the textural characteristics of the support. The purpose of

this study is to see how strongly the location of the metal complex in the structure of the layered material and the properties of supported platinum in the resulting catalyst depend on the structure of the hydroxide precursor of the support.

EXPERIMENTAL

Catalyst Synthesis

The synthesis of the double layered hydroxide $\text{HT}-\text{CO}_3$ by Mg^{2+} and Al^{3+} coprecipitation from dilute nitrate solutions by reacting them with carbonate- and hydroxide-containing solutions was described in detail in our previous publication [12]. For obtaining $\text{HT}-\text{OH}$, the $\text{HT}-\text{CO}_3$ support was calcined at 600°C and was rehydrated at 120°C for 2 h. Before being characterized by physicochemical methods and sorption measurements, $\text{HT}-\text{CO}_3$ and $\text{HT}-\text{OH}$ were dried at 120°C for 12 h.

$\text{H}_2[\text{PtCl}_6]$ was sorbed from aqueous solutions containing an excess amount of the complex at room temperature. The complex concentration in the solution was varied between 2 and 40 mmol/l, depending on the preset metal content of the catalyst. After the sorption of the metal complex, the pH of the remaining solution was measured with a Seven Multi (Mettler Toledo) pH/ion meter, platinum in this solution was quantified spectrophotometrically [13], and the support components—Mg and Al—were determined by atomic absorption spectroscopy on an AA6300 (Shimadzu) spectrometer [14]. The platinum sorption isotherm was obtained using separate samples with a constant support-to-solution weight ratio of 1 : 25.

Catalyst Characterization

Diffuse reflectance spectroscopy (DRS). The diffuse reflectance spectra of supported platinum complexes were obtained on a UV-2501 PC (Shimadzu) spectrophotometer with an ISR-240A diffuse reflectance attachment. The spectra were recorded in the 11000–54000 cm^{-1} range using BaSO_4 as the reference sample and were presented as the Kubelka–Munk function versus wavenumber.

Thermal analysis coupled with mass spectrometry. This method was used to investigate thermal decomposition of pure and platinum-loaded hydrotalcite. Intermediate compounds and decomposition products were analyzed on an STA-449C Jupiter thermal analyzer connected by a heated capillary to a QMS-403C Aeolos (Netzsch) quadrupole mass spectrometer. Measurements were taken in an online mode (argon atmosphere, heating rate of 10 K/min, sample weight of 10–20 mg).

X-ray powder diffraction. X-ray diffraction patterns were recorded on a D8 Advance (Bruker) diffractometer using CuK_α radiation and parallel-beam geometry ($2\theta = 5^\circ$ – 80° , 0.05° increments, counting time of 5 s

per point). High-temperature diffraction patterns were obtained in the 30–900°C range using an HTK 16 (Anton Paar) camera. The measurement conditions are specified in our previous paper [12]. Diffraction data were interpreted using the ICDD database. Structure parameters were calculated using EVA and TOPAS software packages.

Temperature-programmed reduction (TPR). The TPR method was used to study the reduction dynamics of adsorbed metal complexes. The effect of the support on the hydrogen uptake was taken into account by examining chloroplatinate-free samples. Before measurements (AutoChem 2920 instrument, Micromeritics), the sample was purged with flowing helium for 30 min at 25°C and then with a 10 vol % H_2 + Ar mixture (flow rate of 50 ml/min). After the stabilization of the baseline, the sample was reduced while heating to 450°C at a rate of 10 K/min. The gases were 99.99 vol % pure.

Low-temperature nitrogen adsorption. Nitrogen adsorption and desorption isotherms were obtained using an ASAP 2020M (Micromeritics) surface area and porosity analyzer in the equilibrium relative pressure range from 10^{-3} to 0.996 P/P_0 .

The BET specific surface area (S_{BET}) was derived from the adsorption isotherm over the equilibrium nitrogen vapor pressure range of $P/P_0 = 0.05$ –0.25. In the calculation of the specific surface area, we assumed that a nitrogen molecule occupies an area of 0.162 nm^2 in the filled monolayer. The adsorption pore volume (V_{ads}) was determined the amount of nitrogen adsorbed at $P/P_0 = 0.990$ under the assumption that the adsorbate density is equal to the normal liquid density and is 0.808 g/cm^3 . The mean pore diameter was estimated as $D = 4V_{\text{ads}}/S_{\text{BET}}$. The pore size distribution was derived from the desorption isotherm using the Barrett–Joyner–Halenda (BJH) method. The disconnected cylindrical pore model was used in these calculations.

High-resolution transmission electron microscopy (HRTEM). HRTEM images were obtained on a JEM 2010 (JEOL) microscope at a lattice resolution of 0.14 nm and an accelerating voltage of 200 kV. Specimens were prepared by applying ethanolic suspensions onto standard copper grids.

RESULTS AND DISCUSSION

Interaction between $\text{H}_2[\text{PtCl}_6]$ and Aluminum–Magnesium Layered Hydroxides

Sorption processes were investigated for the layered double hydroxides $\text{HT}-\text{CO}_3$ and $\text{HT}-\text{OH}$, which differed in the nature of the interlayer anion. These hydroxides were thoroughly characterized in our earlier work [12]. Sorption curves were obtained for aqueous $\text{H}_2[\text{PtCl}_6]$ solutions in the platinum concentration range of 2–42 mmol/l. Figure 1 demonstrates the marked difference between the chloroplatinate sorption properties of the

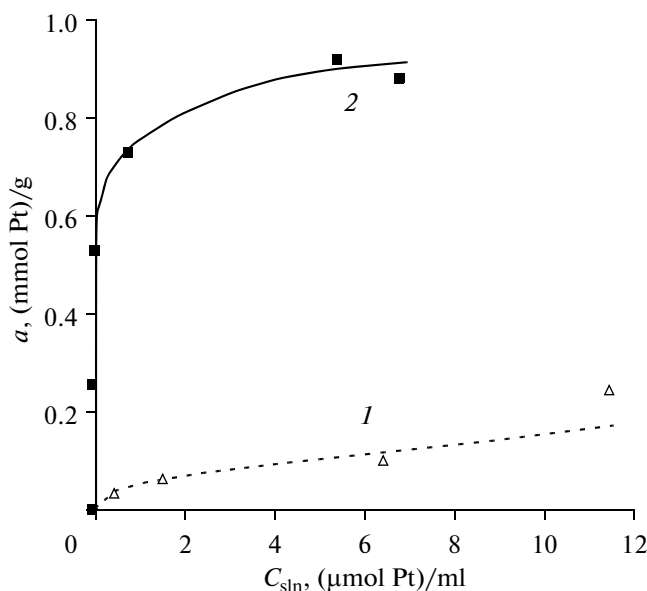


Fig. 1. $[\text{PtCl}_6]^{2-}$ sorption isotherms for the layered aluminum-magnesium hydroxides (1) HT-CO₃ and (2) HT-OH.

supports. In the case of HT-OH, there is a concentration range of strong chloroplatinate adsorption and the maximum amount of adsorbed platinum (18.1 wt %) is close to the stoichiometric value (19.0 wt %) corresponding to the well-known formula of hydrotalcite-like structures ($(M_{1-x}^{2+}M_x^{3+}(\text{OH})_2)^{x+}(\text{A}_{x/m})^{m-} \cdot n\text{H}_2\text{O}$) resulting from the exchange of the interlayer anion A^{m-} for $[\text{PtCl}_6]^{2-}$. Under the same sorption conditions, the HT-CO₃ support binds a much smaller amount of platinum (Fig. 1).

Interacting with the hydroxide support, chloroplatinic acid solutions undergo neutralization to pH 5–10, depending on the acidity of the initial solution. The

aluminum ion concentration in the solution after sorption is at the lower detection limit, while 2 to 7 wt % of the magnesium ions present in the support pass into solution. However, according to X-ray diffraction data, this partial dissolution of magnesium does not break the layered structure and does not cause any significant change in the d_{110} value (1.534 Å), which depends on the Mg : Al molar ratio.

DRS data demonstrated that the chemical composition of adsorbed platinum complexes depends strongly on the nature of the initial hydroxide support. Figure 2 presents the diffuse reflectance spectra of the platinum complexes adsorbed in different amounts on HT-CO₃ and HT-OH. The UV region of the spectrum of the platinum complexes adsorbed on HT-CO₃ (Fig. 2a) shows an intense absorption band at 48400 cm⁻¹ and weaker shoulders at 38000–40000 and 30000 cm⁻¹. These bands are assignable to deeply hydrolyzed platinum species stabilized on the HT-CO₃ surface [16]. The diffuse reflectance spectrum of the platinum complexes adsorbed on HT-OH (Fig. 2b) exhibits three well-resolved absorption bands at 21100, 26600, and 38600 cm⁻¹, indicating that platinum is mainly stabilized as the initial chloro complex [15–17]. Note that, as the platinum content is raised to 10% and above (Fig. 2b, curves 2–4), the 38600 cm⁻¹ band, which is due to the Cl → Pt charge transfer, shifts to a smaller wavenumber of 34400 cm⁻¹, which is possibly explained by the coarsening of the adsorbed particles [18].

An analysis of the data concerning the amount of bound complex and its chemical composition suggests that platinum binds to HT-CO₃ and HT-OH in different ways. According to the present understanding of the structure and properties of aluminum-magnesium hydroxides [19], the anionic platinum chloro complexes can bind to the support by interacting with sur-

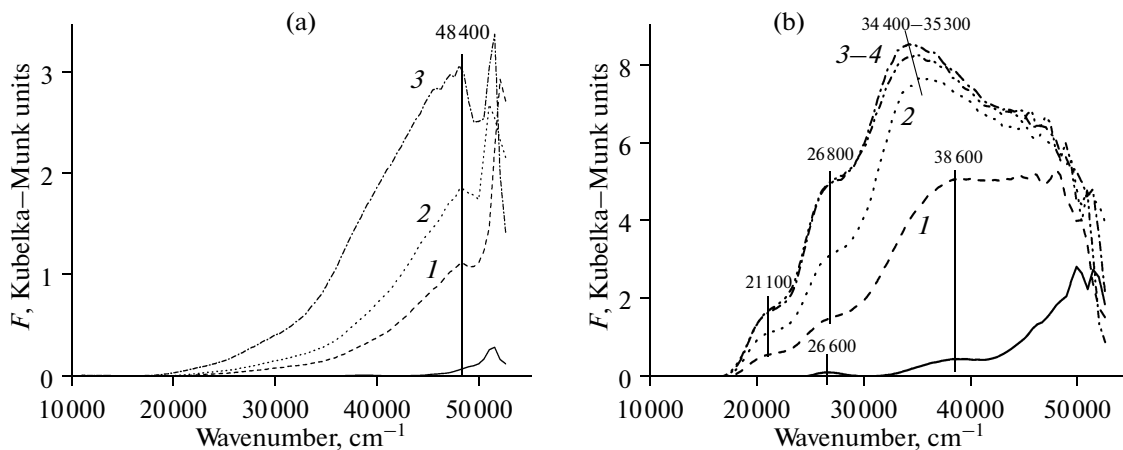


Fig. 2. Diffuse reflectance spectra of the platinum complexes adsorbed on the layered aluminum-magnesium hydroxides: (a) HT-CO₃ with a platinum content of (1) 0.9, (2) 1.8, and (3) 3.5%; (b) HT-OH with a platinum content of (1) 4.9, (2) 10.2, (3) 14.2, and (4) 17.8%. The solid lines are the spectra of the pure supports.

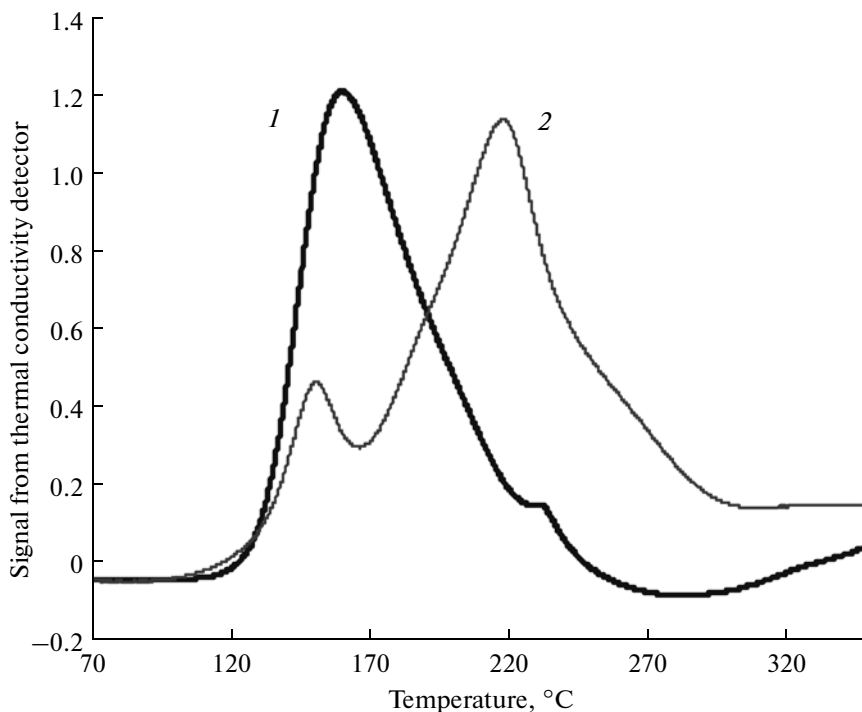
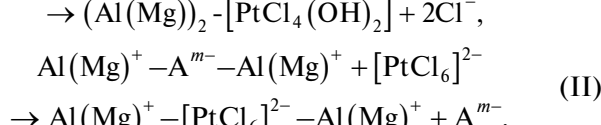


Fig. 3. TPR profiles for the platinum complexes supported on (1) HT-CO₃ (7.8 wt % Pt) and (2) HT-OH (10.2 wt % Pt).

face OH groups (reaction (I)) and by replacing interlayer anions (reaction (II)):



Because of the high pH values in the subsurface layer of the support, the chloro complexes can undergo hydrolysis and platinum can bind as the hydrolyzed species Al(Mg)-PtCl_{6-x}(OH)_x. It is quite possible that insoluble platinum hydroxo complexes also deposit on the surface.

In the case of HT-CO₃, the exchange of interlayer carbonate anions for chloroplatinate ions is likely hampered. This can be due to the equal charges of the CO₃²⁻ and PtCl₆²⁻ anions and, accordingly, similar strengths of the interaction with the aluminum cations of the aluminum-magnesium layers [11, 20]; another possible reason is that this layered support has a more ordered structure [12]. Therefore, the binding of the metal complex to this support will more likely take place via reaction (I), involving surface OH groups.

In the interaction between the chloroplatinate and HT-OH, interlayer OH⁻ anions are readily replaced by the doubly charge complex anion [PtCl₆]²⁻. An additional driving force of this interaction is the neutralization of interlayer OH⁻ anions by hydrogen ions of chloroplatinic acid. When binding to the support in

this way, the chloroplatinate ion does not hydrolyze to any significant extent, and the diffuse reflectance spectrum shows absorption bands characteristic of the platinum(IV) chloro complex.

The finding that the platinum complexes existing on the HT-CO₃ and HT-OH surfaces differ in the way they interact with the support is confirmed by the TPR study of their reduction dynamics. The TPR profiles (Fig. 3) show at least two distinct hydrogen uptake regions, namely, a low-temperature region, with a hydrogen uptake rate peak at 140–160°C, and a high-temperature region, with a hydrogen uptake rate at 220–250°C. The proportions of the corresponding reducible species depend on the nature of the interlayer anion of the support. In the case of HT-CO₃, the dominant platinum species is the “low-temperature” one, which interacts less strongly with the surface. In the case of HT-OH, the reduction of most of the adsorbed platinum occurs above 200°C. It is likely these conditions that ensure the reduction of the platinum(IV) chloro complexes that have been fixed in the interlayer space of the layered support via reaction (II).

Effect of Adsorbed Metal Complexes on the Structure and Thermal Stability of the Layered Aluminum-Magnesium Hydroxides

X-ray diffraction data demonstrate that, for both HT-CO₃ and HT-OH, the basal reflection d_{003} characterizing the layered structure persists upon the binding of the platinum complexes. At the same time,

Table 1. X-ray diffraction data (30°C)

Material	d_{003} , Å	$I(d_{003})$, count/s	h , Å	FWHM*, deg	Crystallite size, Å	a , Å	c , Å
HT-CO ₃	7.84	1484	3.04	0.39	240	3.064	23.54
[PtCl ₆]/HT-CO ₃	7.84	1187	3.04	0.38	250	3.058	23.52
HT-OH	7.72	288	2.92	0.86	110	3.075	23.18
[PtCl ₆]/HT-OH	7.88	173	3.08	1.32	72	3.062	23.64

* FWHM = full width at half-maximum of diffraction peaks.

X-ray diffraction data indicate changes in some structural characteristics of the supports (Table 1). These changes are more pronounced for HT-OH: diffraction peaks become weaker and broader. The broadening of the reflections indicates a decrease in the size of the primary particles (crystallite size) from 11.0 to 7.2 nm. The interplanar spacing d_{003} grows from 0.772 to 0.788 nm, thus increasing the unit cell parameter c from 2.318 to 2.364 nm.

The thermal stabilities of HT-CO₃ and HT-OH loaded with platinum complexes were compared by thermal analysis and high-temperature X-ray diffraction. As is clear from Fig. 4a, the supporting of chloroplatinate on HT-CO₃ does not cause any significant changes in the thermal behavior of the support. The changes in the composition and structure of the material showed themselves as a slight shift of the high-temperature weight loss peak from 420 to 400°C. Investigation of phase transitions in the high-temperature camera of the diffractometer also demonstrated that pure HT-CO₃ and the same material loaded with platinum complexes decompose in similar ways (Figs. 5a, 5b). In both cases, as the temperature is raised, the basal reflection d_{003} shifts from 0.784 to 0.671 nm and, accordingly, the interlayer spacing decreases from 0.304 to 0.191 nm with the formation of the metastable phase $[\text{Mg}_6\text{Al}_2(\text{OH})_{12}\text{O}_2(\text{CO}_3)_x(\text{OH})_y]^0$ between 200 and 375°C [21]. Further heating of the sample yields a periclase-like structure [19].

The binding of the platinum complexes in the interlayer space of the layered structure of HT-OH causes considerable changes in the thermal behavior of the support. According to thermoanalytical data, the amount of interlayer water released in the 200–300°C range increases and the high-temperature DTG peaks change their shapes and positions (Fig. 4b). An appreciable decrease in weight loss is observed in the 340–430°C range, which is associated with the formation of a nonstoichiometric low-temperature spinel phase [12]. The weight loss peak due to the decomposition of the hydroxide phase shifts close to 700°C.

High-temperature X-ray diffraction studies also indicated the effect of the introduction of the metal complex into the HT-OH structure on the thermal behavior of the support (Figs. 5c, 5d). Firstly, the formation of the metastable phase [12] does not take

place in the platinum complex–loaded material, while it is observed in the initial HT-OH, HT-CO₃, and [PtCl₆]/HT-CO₃ (Figs. 5a, 5b). Raising the temperature to 350°C causes only a slight shift of the reflection from the basal plane (003) to larger angles. The corresponding interplanar spacing decreases from 0.772 nm for HT-OH to 0.764 nm for [PtCl₆]/HT-OH because of the elimination of interlayer water. In addition, as distinct from the initial support, [PtCl₆]/HT-OH does not yield the nonstoichiometric spinel phase up to 900°C under our experimental conditions.

The formation of the platinum metal phase in both [PtCl₆]/HT-CO₃ and [PtCl₆]/HT-OH is observed near 700°C (20 = 39.764°, 46.244°, and 67.456°).

Effect of the Metal Complex on the Textural Characteristics of the MgAlO_x Mixed Oxides

The textural characteristics of [PtCl₆]/HT-CO₃ and [PtCl₆]/HT-OH and of the corresponding supports, all calcined at 600°C, are listed in Table 2. Clearly, for both supports, the introduction of platinum causes a slight decrease in the specific surface area and a slight increase in the mean pore diameter.

For HT-CO₃, the introduction of platinum exerts almost no effect on the pore size distribution. An analysis of the pore size distribution curve (Fig. 6a) demonstrates that both oxide phase resulting from the calcination of HT-CO₃ and Pt/HT-CO₃ at 600°C are characterized by a broad pore size distribution with a diffuse maximum. The volume of large pores >20 nm in diameter (macropores and mesopores) is over 2/3 of the entire pore volume.

In the case of HT-OH, the introduction of the platinum complex causes a significant change in the shape of the pore size distribution curve. The proportion of 6–15 nm pores decreases greatly, and mesopores <6 nm in diameter become dominant, accounting for more than 70% of the entire pore volume. Thus, the heat treatment of [PtCl₆]/HT-OH yields an oxide phase with nearly monodisperse pores with a size distribution maximum at 5.5 nm (Fig. 6b).

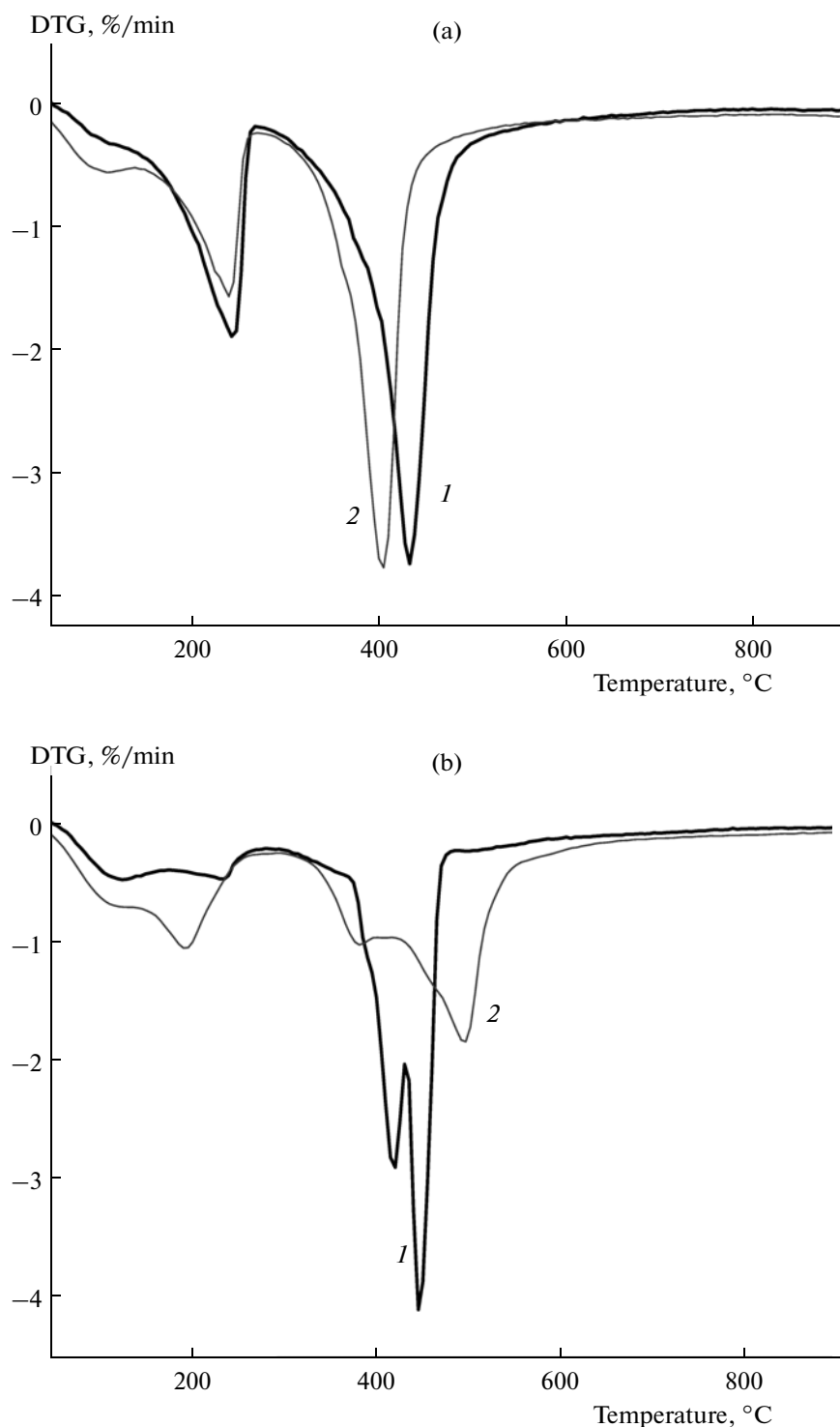


Fig. 4. Thermoanalytical data for the (1) initial supports and (2) supported systems: (a) $[\text{PtCl}_6]/\text{HT-CO}_3$ and (b) $[\text{PtCl}_6]/\text{HT-OH}$.

Effect of the Charge-Compensating Anion of the Layered Supports on the Morphology of Supported Platinum Particles

The platinum complexes in $[\text{PtCl}_6]/\text{HT-CO}_3$ and $[\text{PtCl}_6]/\text{HT-OH}$ were reduced with flowing hydrogen

at 450°C for 2 h. Under these conditions, the reduction reaction was accompanied by the disruption of the layered structure of the support with the formation of an aluminum–magnesium oxide phase. The resulting platinum particles, supported on the mixed oxide, were examined by HRTEM. It was demonstrated that

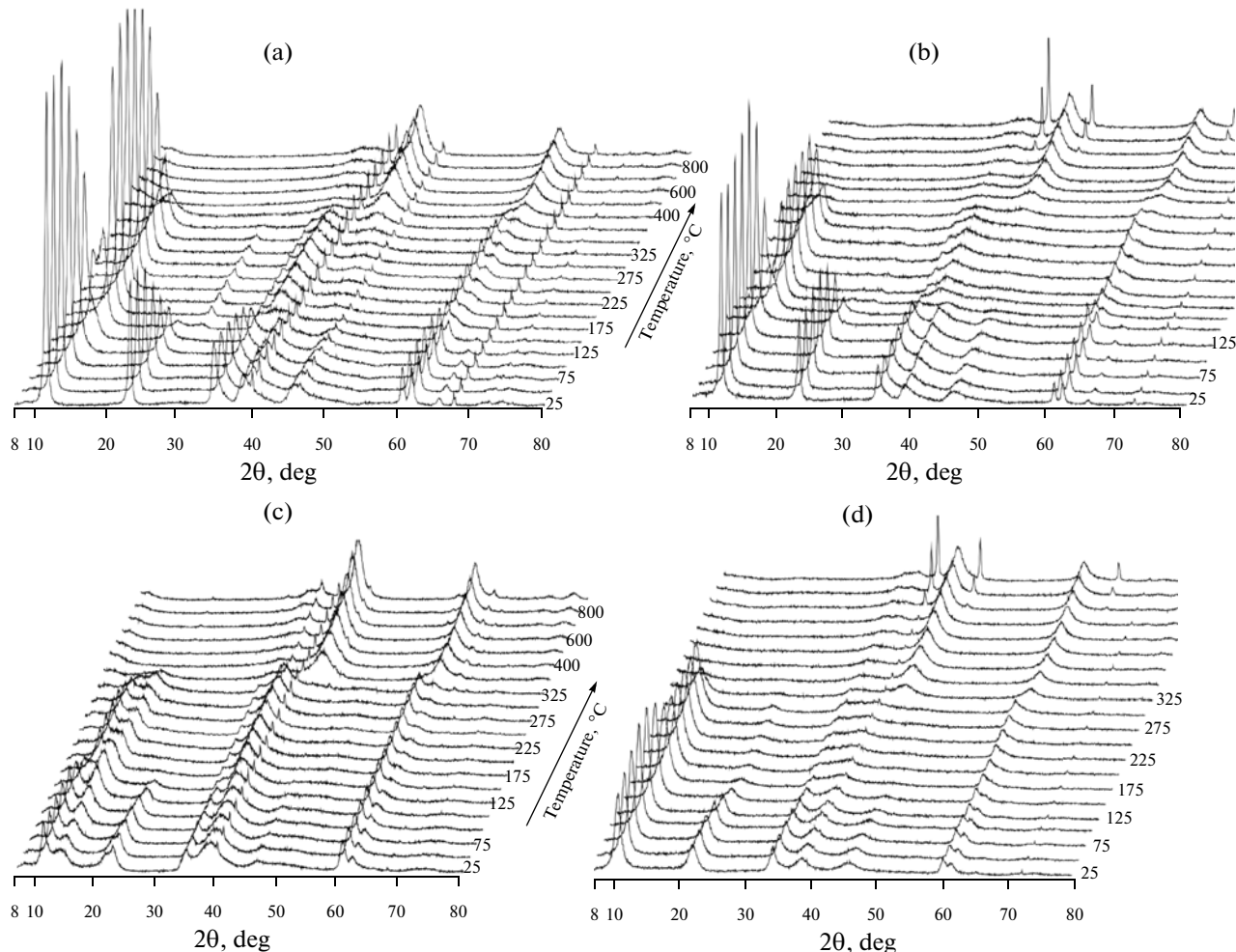


Fig. 5. Variable-temperature X-ray diffraction data (30–900°C) for (a, b) HT-CO₃ and (c, d) HT-OH (a, c) before and (b, d) after [PtCl₆]²⁻ sorption. Platinum content: (b) 7.8 and (d) 10.2 wt %.

heat treatment of the platinum complexes bound to the hydroxide precursor HT-CO₃ yields isometric 2–4-nm platinum particles located on the aluminum–magnesium oxide surface (Figs. 7a, 7b).

In the case of the hydroxide precursor HT-OH, the greater part of platinum in the reduced samples forms

Table 2. Most important textural characteristics of the materials from nitrogen adsorption data (77 K)

Material	S_{BET} , m ² /g	V_{ads} , cm ³ /g	D , nm
HT-CO ₃	229	0.554	9.7
2% Pt/HT-CO ₃	176	0.567	12.9
HT-OH	214	0.318	5.9
4% Pt/HT-OH	188	0.331	7.0

Note: Before measurements, all samples were calcined at 600°C.

larger particles with planar morphology (Figs. 8a, 8b), while the proportion of smaller, isometric particles is insignificant. The extent of the planar particles is up to 50 nm, and their thickness is close to the interlayer spacing $d_{003} = 0.75$ nm in their parent hydroxide HT-OH (Fig. 8b). Platinum was identified as its characteristic interplanar spacing $d_{111} \approx 0.23$ nm. The electron micrographs of the planar platinum particles provide direct evidence for the localization of part of the metal complex inside the layered matrix. An analysis of the HRTEM images and their two-dimensional Fourier transforms (Figs. 8c, 8d) suggests that the particles have a microblock structure and are aggregates of 5- to 10-nm planar fragments. This structure of the particles may result from their growth on several crystallization sites upon the reduction of platinum complexes. The change in the pore size distribution (decrease in the proportion of large pores) that is caused by heat treatment of the Pt-containing sample obtained using the hydroxide precursor HT-OH is apparently due to platinum filling extensive pores to form planar particles.

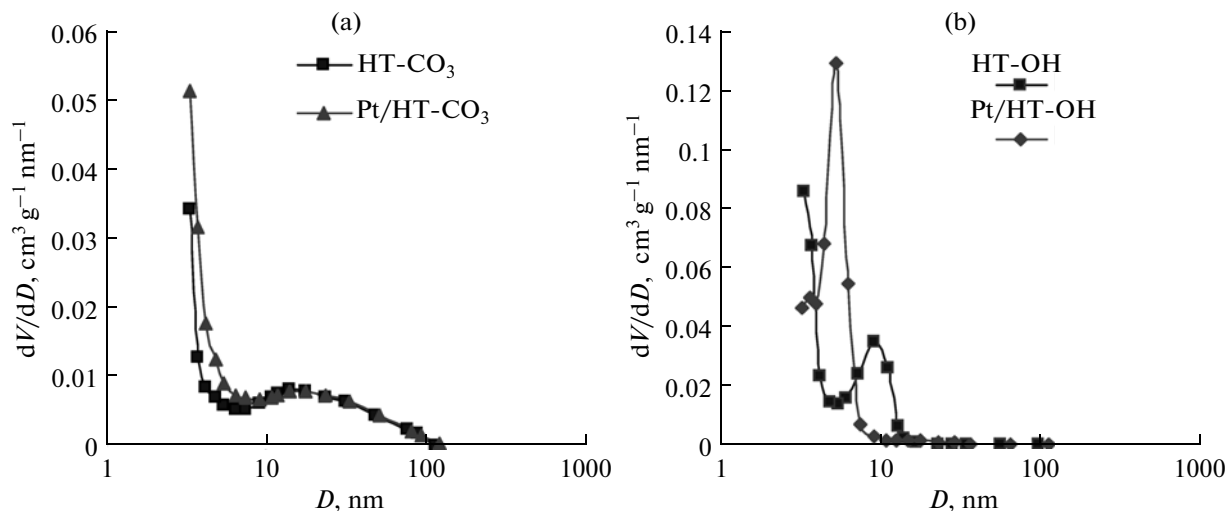


Fig. 6. Pore size distribution curves derived from nitrogen desorption isotherms: (a) Pt/HT-CO₃ and HT-CO₃; (b) Pt/HT-OH and HT-OH. All samples were calcined at 600°C before measurements.

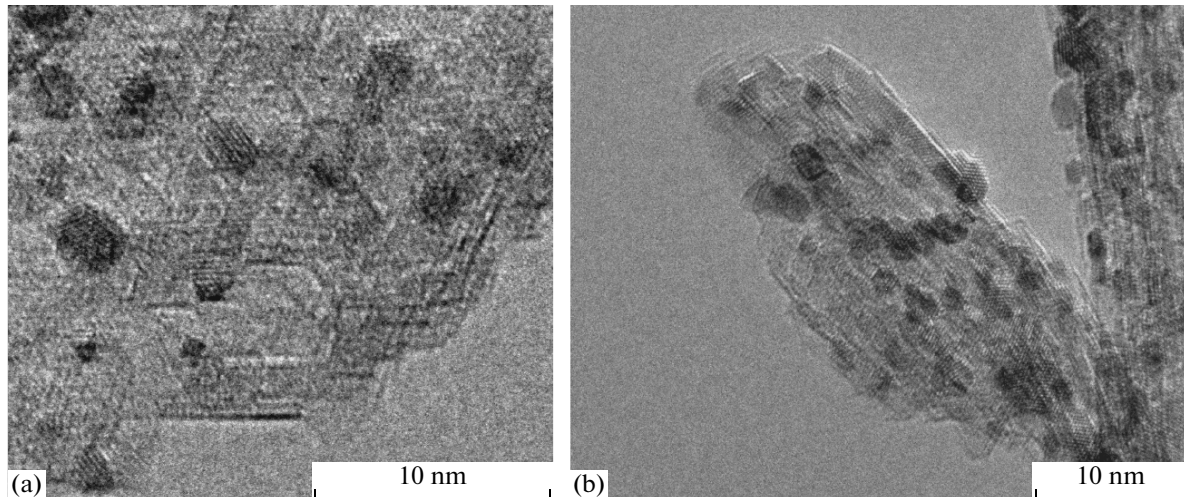


Fig. 7. Electron micrographs of Pt/MgAlO_x (HT-CO₃ precursor, metal content of 7.8%) after reductive treatment at 450°C for 2 h: (a) planar surface and (b) edges of particles.

A study of the interaction of aqueous $\text{H}_2[\text{PtCl}_6]$ solutions with layered aluminum–magnesium hydroxides demonstrated that the structure of the hydroxide precursor (nature of the interlayer anion) is an important factor having an effect on the amount of bound platinum, on the composition of the surface platinum species, and on their location in the layered structure of the material.

In the case of the hydroxide support with the carbonate counterion (HT-CO₃), the introduction of the metal complex exerts no significant effect on the structural properties of the double hydroxide, on the

dynamics of its thermal decomposition, and on the textural characteristics of the resulting oxide phase. Here, the platinum is likely fixed as hydrolyzed species interacting less strongly with the support. This results in the formation of isometric particles 2–4 nm in size.

The binding of the platinum complexes to the aluminum–magnesium hydroxide with interlayer OH[−] anions (HT-OH) increases the interplanar spacing and enhances the thermal stability of the layered structure. In addition, the platinum complexes markedly change the textural characteristics of the support, causing the formation of a nearly monodisperse phase

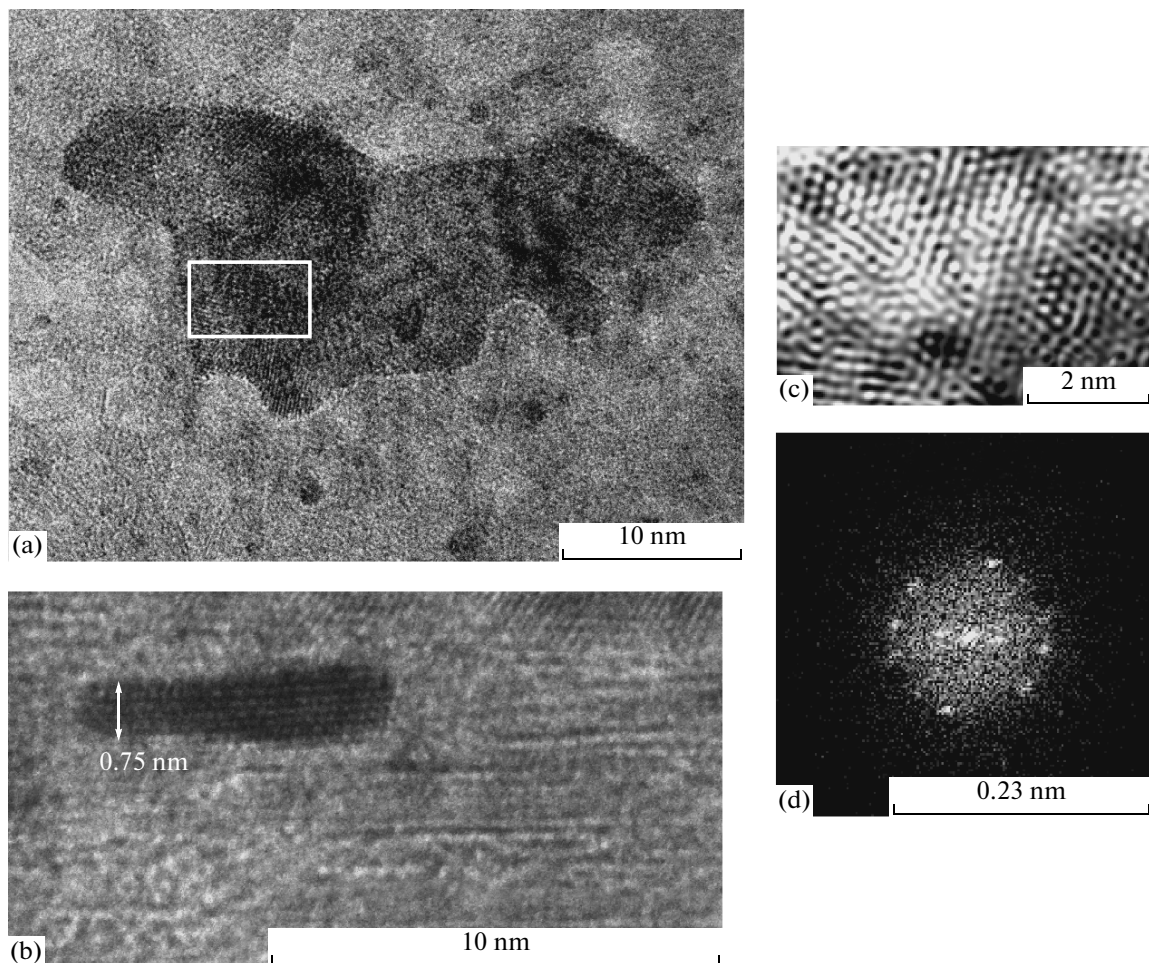


Fig. 8. Electron micrographs of Pt/MgAlO_x (HT-OH precursor, metal content of 10.2%) after reductive treatment at 450°C for 2 h: (a) morphology of a particle of the mixed oxide MgAlO_x containing supported isometric and planar Pt particles; (b) planar Pt particle intercalated in the support matrix (side view); (c) fragment of image (a) (Fourier filtering) showing planes of the Pt crystal lattice; (d) two-dimensional Fourier transform indicating the interplanar spacing $d_{111} \approx 0.23$ nm.

of the mixed oxide. In the Pt/MgAlO_x samples resulting from reductive treatment, a considerable proportion of the platinum is in the form of planar particles. These results are evidence that, at the supporting stage, the metal complexes are largely localized in the interlayer space of HT-OH. In this case, platinum binds to the support as chloro complexes via rapid anion exchange and needs a higher temperature to be reduced.

Thus, the structural difference between the hydroxide precursors enables one to vary the location of the adsorbed metal complex. Accordingly, for a given chemical composition of Pt/MgAlO_x, it is possible to obtain platinum particles differing radically in their size and morphology. We are going to continue this study by investigating the electronic state and catalytic properties of the uncommon, planar platinum particles that form in the confined spaces of the layered structure.

ACKNOWLEDGMENTS

The authors are grateful to T.P. Sorokina for providing a layered double hydroxide sample and to N.V. Antonicheva for carrying out thermal analyses.

This work was supported by grant no. NSh-5797.2008.3 from President of the Russian Federation.

REFERENCES

1. Cabello, F.M., Tichit, D., Coq, B., Vaccari, A., and Dung, N.T., *J. Catal.*, 1997, vol. 167, p. 142.
2. Tichit, D., Durand, R., Rolland, A., Coq, B., Lopez, J., and Marion, P., *J. Catal.*, 2002, vol. 211, p. 511.
3. Silletti, B.A., Adams, R.N., Sigmon, S.M., Nikolaopoulos, A., Spivey, J.J., and Lamb, H.H., *Catal. Today*, 2006, vol. 114, p. 64.
4. Centi, G. and Perathoner, S., *Catal. Today*, 2007, vol. 127, p. 219.

5. Fornasari, G., Glockler, R., and Vaccari, A., *Appl. Clay Sci.*, 2005, vol. 29, p. 258.
6. Gerardin, C., Kostadinova, D., Sanson, N., Francova, D., Nanchoux, N., Tichit, D., and Coq, B., *Stud. Surf. Sci. Catal.*, 2005, vol. 156, p. 357.
7. Gando, Z., Coq, B., Menorval, L.C., and Tichit, D., *Appl. Catal., A*, 1996, vol. 147, p. 395.
8. Lukashin, A.V., Chernysheva, M.V., Vertegel', A.A., and Tret'yakov, Yu.D., *Dokl. Chem.*, 2003, vol. 388, nos. 1–3, p. 19.
9. Chang, C.T., Liaw, B.J., Huang, C.T., and Chen, Y.Z., *Appl. Catal., A*, 2007, vol. 332, p. 216.
10. Albertazzi, S., Busca, G., Finocchio, E., Glockler, R., and Vaccari, A., *J. Catal.*, 2004, vol. 223, p. 372.
11. Miyata, S., *Clays Clay Miner.*, 1983, vol. 31, no. 4, p. 305.
12. Bel'skaya, O.B., Leont'eva, N.N., Gulyaeva, T.I., Doronin, V.P., Zaikovskii, V.I., and Likhobolov, V.A., *Kinet. Catal.*, 2011, vol. 52, no. 5, p. 761.
13. Ginzburg, S.I., Gladyshevskaya, K.A., Ezerskaya, N.A., et al., *Rukovodstvo po khimicheskому analizu platinovykh metallov i zolota* (Guide to Chemical Analysis of Platinum Metals and Gold), Moscow: Nauka, 1965.
14. Yudelevich, I.G. and Startseva, E.A., *Atomno-absorbtionnoe opredelenie blagorodnykh metallov* (Atomic Absorption Spectroscopy for Determination of Noble Metals), Novosibirsk: Nauka, 1981.
15. Bel'skaya, O.B., Karyanova, R.Kh., Kochubei, D.I., and Duplyakin, V.K., *Kinet. Catal.*, 2008, vol. 49, no. 5, p. 720.
16. *Analiticheskaya khimiya platinovoi gruppy* (Analytical Chemistry of the Platinum Group), Zolotov, Yu.A., Ed., Moscow: KomKniga, 2005.
17. Bel'skaya, O.B., Maevskaia, O.V., Arbuzov, A.B., Kireeva, T.V., Duplyakin, V.K., and Likhobolov, V.A., *Kinet. Catal.*, 2010, vol. 51, no. 1, p. 98.
18. Basile, F., Fornasari, G., Gazzano, M., and Vaccari, A., *Appl. Clay Sci.*, 2000, vol. 16, p. 185.
19. Cavani, F., Trifiro, Fr., and Vacari, A., *Catal. Today*, 1991, vol. 11, p. 173.
20. He, J., Wei, M., Li, B., Kang, Y., Evans, D.G., and Duan, X., in *Layered Double Hydroxides, Structure and Bonding*, vol. 119, Berlin: Springer, 2006, p. 89.
21. Stanimirova, T., Vergilov, I., Kirov, G., and Petrova, N., *J. Mater. Sci.*, 1999, vol. 34, p. 4153.